Reports on Geodesy and Geoinformatics, 2022, Vol. 113, pp. 1–10

DOI: 10.2478/rgg-2022-0001
Received: 9 December 2021 / Accepted: 11 January 2022
Published online: 27 May 2022

ORIGINAL ARTICLE

Research of the environmental temperature influence on the horizontal displacements of the Dnieper hydroelectric station dam (according to GNSS measurements)

Kornyliy Tretyak [1*] and Bohdan Palianytsia [1]

[1]Department of Higher Geodesy and Astronomy, Lviv Polytechnic National University, 12, Stepan Bandera Str., Lviv, 79013, Ukraine

[*]kornylii.r.tretiak@lpnu.ua

Abstract

The paper studies the relationship between the ambient temperature change and the horizontal displacements on control points of the Dnieper Hydroelectric Station dam from 2016 to 2020. A specially developed software product analyzed the GNSS time series of measurements pre-processed by the GeoMoS system to determine the parameters of seasonal displacements and their relationship with seasonal changes in air temperature. The research established that the influence of ambient temperature in the absence of significant changes in the water level in the upper reservoir determines the cyclicity of dam deformations. It is established that the projections of velocity vectors of reference points in the ETRF-2014 system for the studied period do not exceed the absolute value of 3 mm/month. The directions of the horizontal displacement vectors in the first half of each year are opposite to the directions recorded in the second half. In the first half of the year, the dam's body shifts towards the reservoir, while in the second half year period, it shifts-backwards. According to the three-year GNSS monitoring of the Dnieper Hydroelectric Station dam, the amplitude of semi-annual horizontal oscillations of the control points relative to the dam axis is from -9.5 to +8 mm. In winter and summer, the horizontal displacements increase from the edges of the dam to its central part, and the amplitudes of the horizontal displacements move vice versa. The obtained data establish a linear analytical relationship between the average temperature and the horizontal displacements of the GNSS control points.

Key words: GNSS measurements, geodetic monitoring of hydraulic structures, seasonal deformations of the dam, geodetic monitoring of the Dnieper Hydroelectric Station.

1 Introduction

Monitoring hydroelectric dams is an essential tool for assessing their stability and integrity. Many dams of large hydropower plants have developed comprehensive monitoring programs that use modern methods of integrated analysis (factors that impair the stability of these objects) and modelling deformation processes. Such programs are based on the use of reliable control and measuring equipment and full automation of measuring various physical parameters, as well as the collection of data. The result is a time series of changes in these parameters. It is essential to properly study these time series and understand the physics of the processes, their mechanism and explain the causes of deformations. Automation of monitoring data collection allows taking a comprehensive approach to dam deformation monitoring. It is possible to combine geotechnical and geophysical monitoring tools.

Reliability is a crucial monitoring requirement, as a poorly designed monitoring scheme can lead to erroneous conclusions and

Publisher: De Gruyter

misinterpretation of ongoing processes. A reliable monitoring scheme is based on the following aspects:

- correct understanding of the processes that cause deformations;
- identification of sources of measurement errors in monitoring tools and their consideration;
- sufficient redundant observations to balance them;
- resistance of the dam to adverse environmental conditions.

One of the methods of assessing the stability of the dam is geodetic monitoring. The structural complexity of these engineering constructions requires a careful approach to creating a monitoring system. The purpose of monitoring is to prevent severe accidents and damage and collect data to verify design parameters, study the causes of deformation processes, and gain experience to create new, more advanced projects (Chrzanowski et al., 2011).

Methods based on Global Navigation Satellite Systems (GNSS) were initially widely used to measure displacements at dam points. Later, GNSS networks were created to be used for periodic measurements at controlled reference points. In recent years, automated control systems (ACS) and integrated geotechnical systems have been developed. Automated receivers obtain signals from the GNSS capable of operating in a continuous mode. And integrated receivers together with other means of monitoring are included in the system of early warning of threats to the safe operation of hydraulic structures (Drummond, 2010; Milillo et al., 2016; Scaioni et al., 2018). Analysis and interpretation of deformation processes at hydropower facilities actively use the obtained integrated data.

Monitoring data are also used to study the response of dams to water levels changes in the reservoir, seasonal changes in environmental conditions, including temperature, etc. (Chrzanowski et al., 2011; Corsetti et al., 2018).

Studies of the impact of changes in ambient temperature on large engineering structures, including hydroelectric dams, are especially relevant in global climate change, which has been actively occurring in recent years.

A number of authors (Mata et al., 2013; Oro et al., 2016; Zhang et al., 2018, and others) argue that one of the leading causes of seasonal deformation of dams is the dynamics of the annual change in air temperature, provided that the water level in the reservoir does not change significantly.

In order to assess the impact of annual changes in air temperature on the deformation of the dam, researchers used a variety of mathematical approaches and took into account the design features of hydraulic structures. For example, in Oro et al. (2016), correlation analysis and methods of multifactor analysis were used to assess the impact of environment and temperature, in particular on the displacement of structures and foundations of dams. The displacements of concrete were determined from measurements by pendulums and extensometers, considering the influence of the environment. The temperature of the concrete surface, the ambient temperature and the water level in the reservoir were taken into account.

A significant challenge in developing an accurate model for predicting dam behaviour is modelling the effect of possible extreme temperature values. Kang and Li (2020) presents a model of dam deformation based on Gaussian regression to monitor the condition of concrete gravity dams, which can model the temperature effect using long-term air temperature data. The obtained results show that models based on Gaussian regression can reflect the effect of extreme air temperature on the displacement of concrete gravity dams.

In Kuzmanovic et al. (2013), a 3D-numerical model was developed to analyze non-stationary stepwise thermal stress in HPP dams. The model was tested, relying on field studies of the Platanovrissi dam, built on the river Nestos in Greece. The relationship between temperature, monolith length and tensile stresses of the gravity dam was analyzed.

A sinusoidal function, whose argument is the ordinal number of the day from the beginning of the year to the observation date, represents the annual variation of the Alto Lindoso concrete dam in Portugal (length 297 m, height 110 m) and the effect of changes in concrete temperature in Mata et al. (2013). It is established that the study of the influence of the daily change of air temperature on the reaction of a concrete dam contributes to a better investigation of its constructive behaviour. In dams with automated data acquisition systems, the temperature effect of the wave with diurnal fluctuations can be used to predict and detect anomalous behaviour. The ratio obtained by the authors can be used to assess whether there are changes in the response of the dam to short-term loads, corresponding to the analyzed daily fluctuations.

Studies of the dynamics of the Ermenek dam, which is the second-highest dam in Turkey (length - 123 m, height - 218 m), were conducted based on geodetic measurements and analysis of the finite element model during the first period of operation, i.e., from the end of construction to complete tank filling (Yigit et al., 2016). We researched the response of the dam to changes in the reservoir level in the upper reaches and seasonal temperature fluctuations. Correlation analysis of the obtained time series showed that the periodic and linear displacements of the dam are associated with changes in seasonal temperature and increasing water level, respectively, which indicates the relationship between temperature, water load and deformation of the dam.

Arched dams, which are much thinner than concrete gravity dams, respond somewhat differently to seasonal temperature fluctuations and therefore require other approaches to determine the effects of such influences. In Léger and Leclerc (2007), it is proposed to describe the heat transfer equations as an example of temperature change in the sections of arched dams. The authors developed algorithms for calculating the spatial distribution of temperature and its time change over time for the "direct" problem, where temperature fluctuations are set at the ascending and lower flow faces. Algorithms were also developed for the "reverse" problem, where temperature was measured directly by thermometers inside dam sections. The resulting nonlinear temperature field was decomposed into the effective mean and linear temperatures. The difference between these values was compared with the reaction of the dam.

The results of monitoring the arch dam of Lijiaxia HPP (main section length 204 m, height 147 m) located on the Chinese Yellow River did not reveal correlations between dam deformations and reservoir level fluctuations (Zhang et al., 2018). Only seasonal temperature changes were the main factor of those correlations. It was found that when the temperature reached its highest value in July 2015, the arched dam expanded, moving upstream, and its creep became maximum. In January, however, the dam was compressed, moving downstream. The displacement in the middle was about 10 mm, and at the edges - about 5.3 mm.

Kang and Li (2020) presents a Gaussian regression displacement model for monitoring the stability of concrete gravity dams, which can model the temperature effect using long-term air temperature data.

The study Oro et al. (2016) uses Correlation analysis and methods of multifactor analysis to assess the impact of the environment on the displacement of structures and foundations of dams. The displacements of concrete were determined from measurements by pendulums and extensometers, considering the influence of the environment. The temperature of the concrete surface, the ambient temperature and the water level in the reservoir were taken into account.

Studies on arched dams performed in Santillán et al. (2015) showed that heat loads, compared to others, have the most significant impact on the formation of cracks. In addition, as global climate change studies indicate the growth of the average temperature on the Earth, it is important to assess the impact of future temperature increase on the construction behaviour of sensitive infrastructures. This paper proposes a methodology for assessing

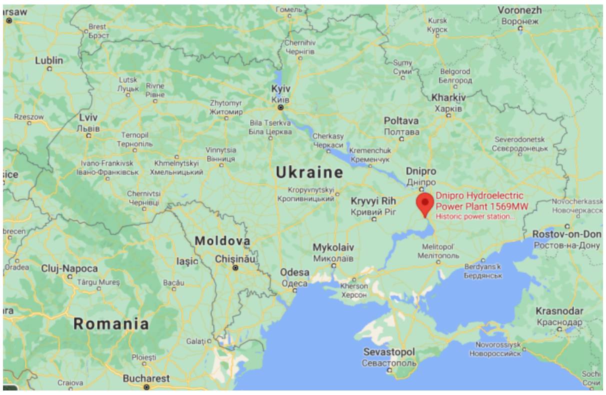

Figure 1. Location of the Dnieper Hydroelectric Station

Figure 2. General view of the Dnieper Hydroelectric Station from the right bank

the impact of global warming on the structural behaviour of the dam. Researchers link future climate scenarios to thermal, stress, and landslide fields. It is indicated that raising the concrete temperature to 5.6 ^{0}C can cause an increase in the average annual radial displacement in some cases, even more than 100%. The example of the arch dam La Baells (Spain) illustrates the methodology.

Léger and Leclerc (2007) proposes to describe temperature changes in the cross-sections of arched dams by heat transfer equations. Algorithms have been developed to calculate the spatial distribution of temperature and its time change for the "direct" and "reverse" problems. In the "direct" problem, temperature fluctuations are set at the ascending and lower sides of the flow. In the "reverse" problem, the temperature was measured directly by thermometers located inside dam sections. The resulting nonlinear temperature field was decomposed into effective mean and linear temperatures. The difference between these values was compared with the reaction of the dam.

Studies of the influence of temperature on the stability of hydraulic structures are relevant in Ukraine because of developing hydropower at a high level. There are six hydro units on the Dnieper River alone, the most powerful of which is the Dnieper Hydro Unit, located near the city of Zaporizhia (Figure 1). The dam of the Dnieper Hydroelectric Station belongs to the dams of the massive buttress type.

The basis of the Dnieper Hydroelectric Station buildings (Figure 2) is crystalline rocks of the Zaporizhzhya block, represented mainly by weakly weathered cracked granites and granite gneisses. Tectonic cracks and deep faults dissected the crystalline massif, and it is broken by several systems of cracks separately. A characteristic feature of the longitudinal and transverse cracks of the array is their considerable length and endurance direction (Tretyak and Palianytsia, 2021). The bottom and banks of the river valley in this area form an array of medium- and coarse-grained Archean granites.

Figure 3. View from the Dnieper Hydroelectric Station's left bank after the destruction on August 18, 1941 (Photo from the Central State Archive of Ukraine)

Construction of the power plant began in 1927, and in 1932 it was brought into operation. The length of the dam was 760 m, height - 60 m.

The history of the dam was not accessible. It was destroyed twice during World War II (in 1941 and 1943) (Moroko, 2010). Figure 3 shows the dam of the Dnieper Hydroelectric Station ruined by the explosion. The middle part of the dam, which was closer to the right bank of the Dnieper, suffered most.

In 1944, the reconstruction of the hydroelectric power plant began. In 1947, the first unit of the Dnieper Hydroelectric Station was put into operation. Seventeen turbines are operating today.

It is essential to monitor the technical condition of the dam constantly to prevent the negative consequences of large-scale destruction and ensure the reliable operation of hydropower plants. Among the methods of dam stability control, geodetic monitoring occupies a vital place. The complexity of the design of hydraulic structures that are part of the Dnieper Hydroelectric Station requires creating a modern automated monitoring system using space technology. Monitoring of spatial displacements by GNSS methods has started here since 1997. The analysis of the results of the observations indicated the possible presence of cyclic seasonal displacements of the crest of the Dnieper Hydroelectric Station dam. Studying these movements and accumulating relevant data requires constant monitoring of various physical indicators and different geodetic measurements (Tretyak et al., 2015). At the Dnieper Hydroelectric Station, in 2015, Leica Geosystems installed a stationary system for monitoring the spatial displacements of buildings, which led to a significant increase in efficiency and automation of data acquisition. This system uses the Spider software to quickly collect, pre-process and transmit to the server the results of measurements from monitoring devices installed on the dam. Leica GMX902 GG multisystem GNSS receivers are equipped with AR10 antenna, TM30 total robotic stations, Nivel 201 precision inclinometers and DTM meteorological sensor. In the future, the GeoMoS software product will perform joint processing of the obtained data.

2 The purpose

The purpose of the study is to investigate the relationship between the horizontal displacements of GNSS control points on the dam of the Dnieper Hydroelectric Station based on data obtained by an automated monitoring system and changes in ambient temperature in the period from 2016 to 2020.

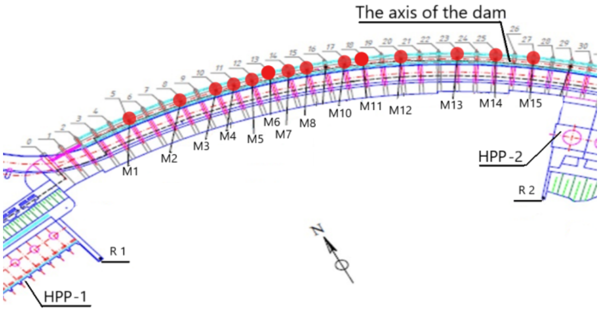

Figure 4. Diagram of the location of GNSS control points MP1-MP15 on the dam of the Dnieper Hydroelectric Station

Figure 5. General view of checkpoints (including MP-4)

3 Output data

The research used the GNSS data of measurements carried out at the points of the Dnieper Hydroelectric Station dam. Figure 4 shows the location of the items. Directly on the dam, there are 16 checkpoints (MP1-MP16), where round-the-clock GNSS observations are carried out (from point MP-9, the information was not received, and point MP16 is outside the investigated part of the dam), and two fundamental geodetic points R1 and R2, equipped GNSS receivers Leica GMX902 GG with antenna AR10. The general view of the checkpoint MP-4 is presented in Figure 5.

The research used only GNSS measurement data obtained from the beginning of the installation of the automated control system in the period from 09.02.2016 to 12.07.2020 with a recording frequency of 30 s. The initial data turned out to be unreliable, as the system was debugged during that period of operation. Therefore, calculations used the data obtained after July 2016. Other terrestrial geodetic measurements conducted at the station do not correspond to the accuracy of GNSS measurements, so the studies were not taken into account.

4 Research results

Analysis of time series of change of the points coordinates defined by the GNSS method established gross errors in the measurements processed by the GeoMoS software package. It was especially evident at the setting up of the system and when replacing equipment. Accordingly, these data required filtering. Data filtering is necessary because cranes operate on the dam, limiting the visibility of satellites and creating multi-path propagation of signals from satellites. Therefore, there will be no solutions or gross errors in many cases.

The research of time series established that the average maximum value of the displacement in the horizontal plane and height relative to the average position of the point for the whole period does not exceed 20 mm. Values of deviations from the mean position of the point, exceeding the absolute value of 60 mm, were filtered according to the 3D rule. The second step of filtering was to determine the average maximum offset for the entire period separately for each point. Repeated filtration eliminated offsets that were greater than three times the mean maximum offset in absolute terms.

The filtered data determined almost daily displacements of all GNSS points during the entire observation period. The amplitude of oscillations at each point is different, but the displacement curves have a typical pattern. It consists in the fact that the displacements have a smooth harmonic character during each year, and extreme deviations relative to the axis of the dam are recorded annually in February (corresponding to 0.1 years from the beginning of the year) and in August (corresponding to 0.6 years from the beginning of the year). Thus, the displacements are almost linear during the six-month periods (approximately from February to August). Usually the offset of GNSS points is not linear, but every six months, there is a change in the direction of point offset to the opposite. According to GNSS measurements, the length and direction of the displacement vector for each point for six months are determined. Relevant determinations have been made for average speeds.

Daily solutions for items MP1–MP15 were obtained from processing the GNSS measurements for the entire observation period. All daily solutions were jointly processed in the Bernese ADDNEQ2 program, and the final coordinates and velocities of the stations were calculated and reduced to the middle epoch each time series.

For example, Table 1 shows the displacement velocities of GNSS control points of the Dnieper Hydroelectric Station and the estimation of velocity accuracy for one of the spring-summer periods (2018.1–2018.6) and one of the autumn-winter periods (2018.6–2019.1). The velocities of the control points are given in the topocentric coordinate system (directions N – north; E – east; U – up).

The projections of the velocity vectors of the reference points in the ETRF-2014 system do not exceed the absolute value of 3 mm/month. The average speed of displacement of control points installed on the dam is 1.4 mm/month in the northern and eastern directions.

Figure 6 shows a graphical representation of the distribution of velocity vectors of horizontal displacements of points for specific semi-annual periods from 2017 to 2020. It illustrates the opposition between the horizontal vectors in the first and the second half of each year. In the first half of the year, the dam's body shifts towards the reservoir. In the second half year period, it moves in the direction of the lower reaches.

According to the following expression, an approximation of their displacement was performed to determine the average amplitudes and periods of displacement of all control points throughout the observation period:

$$\Delta(T)_i = a_0 + a_1 \cdot \cos\left(\frac{T_i}{T}\right) + a_2 \cdot \sin\left(\frac{T_i}{T}\right) \qquad (1)$$

where: a_0, a_1, a_2 – approximation coefficients, T_i – serial number of the day from the beginning of the year, T – number of days in 1 year.

In order to establish the spatial and temporal relationship between the horizontal displacements of the dam control points and the average air temperature, we analyzed the changes in the annual air temperature near the dam during 2017–2019 and calculated the average temperature values. Air temperature data at the Dnieper Hydroelectric Station came with a discreteness of 3 hours, starting from 2 hours to 23 hours each day. During the year, there were 2920 temperature measurements. Figure 7 shows the change in temperature during the study period.

Next, the average value of the temperature was calculated by using the trapezoidal formula to solve the integral.

In the beginning, the average values of temperature for the entire period, i.e., from 2016 to 2021, were calculated, consistently taking into account each subsequent measurement. The obtained

Table 1. Displacement speeds of GNSS control points of the Dnieper HPP for the period from 2018.1 to 2019.1

Point name	Measurement period 2018.1 - 2018.6						Measurement period 2018.6 - 2019.1					
	Displacement rates			Displacement rates error			Displacement rates			Displacement rates error		
	V_E	V_N	V_U	m_{VE}	m_{VN}	m_{VU}	V_E	V_N	V_U	m_{VE}	m_{VN}	m_{VU}
	[mm/month]			[mm/month]			[mm/month]			[mm/month]		
MP-1	-0.95	1.11	0.90	0.17	0.17	0.28	0.58	-2.03	-0.61	0.07	0.10	0.07
MP-2	-0.91	0.34	-0.06	0.32	0.37	0.36	0.07	-2.19	-0.37	0.15	0.15	0.29
MP-3	-1.28	1.91	0.79	0.09	0.11	0.09	0.48	-2.30	-0.47	0.09	0.08	0.09
MP-4	-1.19	1.56	0.97	0.06	0.08	0.09	0.22	-1.99	-0.69	0.06	0.09	0.08
MP-5	-0.75	1.30	1.41	0.06	0.09	0.10	-0.05	-1.59	-0.80	0.05	0.07	0.07
MP-6	-1.12	1.65	1.39	0.07	0.07	0.09	0.13	-1.80	-0.88	0.06	0.09	0.07
MP-7	-0.42	1.61	1.44	0.08	0.09	0.10	-0.56	-2.00	-0.91	0.06	0.10	0.09
MP-8	-0.72	1.75	1.34	0.06	0.10	0.08	-0.17	-2.14	-0.97	0.06	0.07	0.10
MP-10	-0.82	1.80	1.27	0.06	0.09	0.10	-0.28	-2.06	-0.87	0.05	0.12	0.09
MP-11	-0.45	1.75	0.96	0.07	0.10	0.11	-0.44	-2.25	-0.65	0.04	0.09	0.07
MP-12	-0.36	1.82	1.02	0.11	0.11	0.10	-0.62	-2.11	-0.69	0.06	0.07	0.07
MP-13	-0.25	2.61	0.91	0.07	0.10	0.11	-0.77	-3.07	-0.67	0.08	0.12	0.26
MP-14	-0.38	2.43	1.13	0.08	0.13	0.10	-0.60	-2.63	-1.00	0.04	0.10	0.10
MP-15	-0.44	2.14	0.98	0.06	0.09	0.11	-0.66	-2.39	-0.60	0.04	0.09	0.07

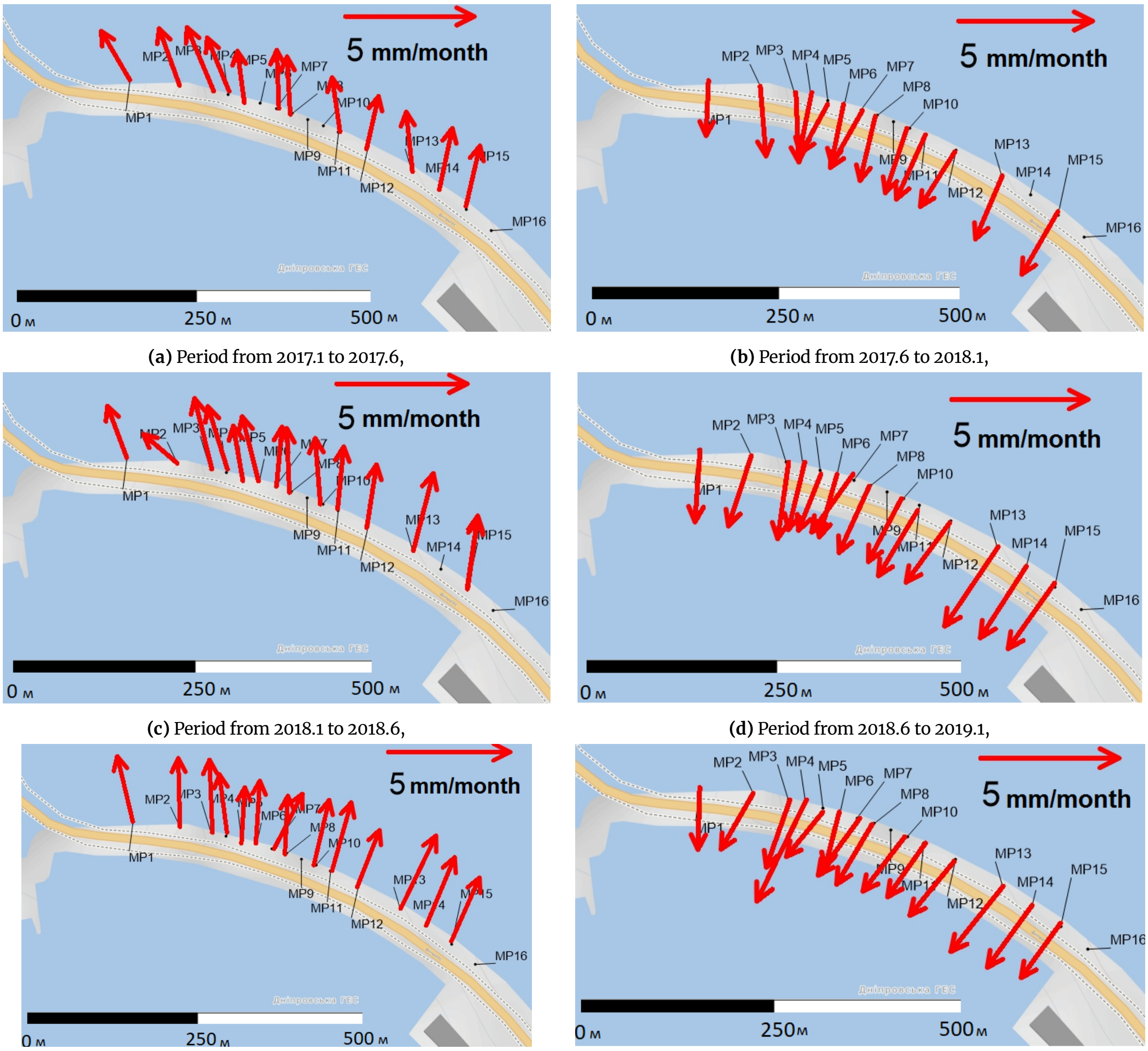

(a) Period from 2017.1 to 2017.6,
(b) Period from 2017.6 to 2018.1,
(c) Period from 2018.1 to 2018.6,
(d) Period from 2018.6 to 2019.1,
(e) Period from 2019.1 to 2019.6,
(f) Period from 2019.6 to 2020.1.

Figure 6. Distribution of velocity vectors of control points horizontal displacements of the Dnieper Hydroelectric Station dam from 2017.1 to 2020.1

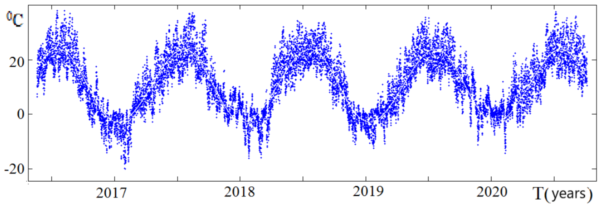

Figure 7. Temperature changes from 2016 to 2020 (according to the Dnieper Hydroelectric Station meteorological station)

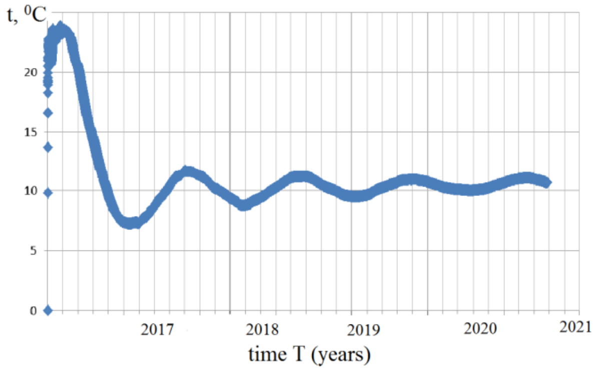

Figure 8. Average values of temperature (with accumulation) in the period from January 2016 to September 2019

results allowed a possibility to construct a graph with the epoch (year) on the abscissa axis and the mean integral value of temperature in °C on the ordinate axis (Figures 8–9). The temperature curve in the Figure 8 asymptotically approaches the value of about 10°C. Approximately the same temperature value is fixed in the lower groove and the concrete thickness of the dam.

The annual report 'Action Plan for Adaptation to the Consequences of Climate Change in the City of Zaporizhia' (2020) states that the analysis of the average annual air temperature in Zaporizhia for 30 years (1989–2018) and its deviation from the climatic norm showed that its values increase during the specified period. The average annual air temperature in Zaporizhia from 1989–2018 was +9.9°C, which is 0.5°C higher than the forecast norm, which is +9.4°C.

Studies show that Ukraine's climate has begun to change significantly in recent decades (temperature and some other meteorological parameters differ from climatic norms). According to the simulation results, Ukraine's air temperature will continue to rise in the future (although the magnitude of changes varies slightly in different forecast models). Furthermore, there will be a change in precipitation during the year. It confirms the relevance of research on the effect of temperature on the stability of the Dnieper Hydroelectric Station dam.

Further integration was performed at each point for the previous annual period and the Figure 9 was obtained. The peculiarity of this curve is that the average value for the annual period will be close to the average annual temperature value for a given region, which is about 10°C. The graph shows a small temperature range on the y-axis from 9°C to 11.5°C and the irregularity of its change.

In the following calculations, the integration period decreased: six months, four months, three months, two months and one month. Figure 9 shows graphs of changes in average temperature, where its integration was carried out for previous periods of different duration, namely: in Figure 10a half-year period, Figure 10b three-month and Figure 10c monthly, respectively. The research used data on temperature changes during seven years from 2014 to 2020 inclusive. The plots represent the temperature value on the ordinate axis and the ordinal number of this value for the corresponding period on the abscissa axis.

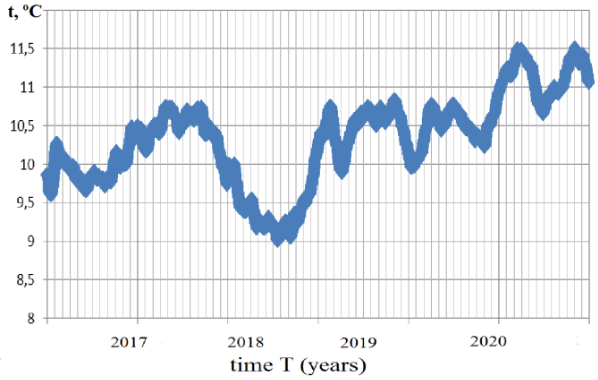

Figure 9. Annual average values of temperature in the period from 2016-2021

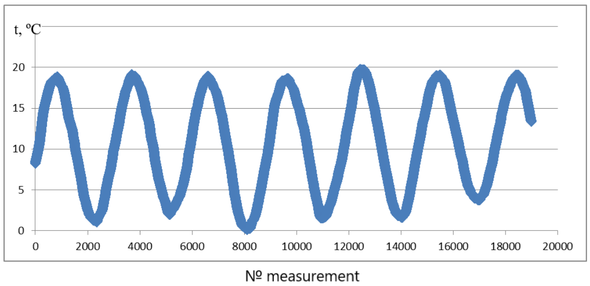

(a) 6 months

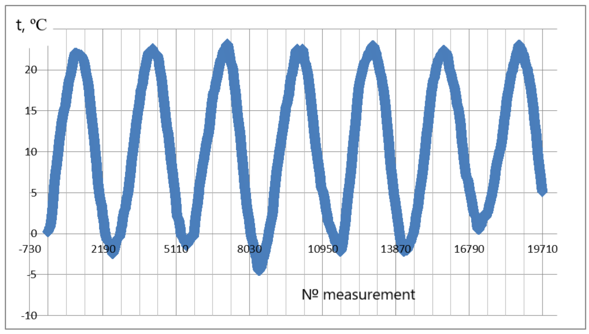

(b) 3 months

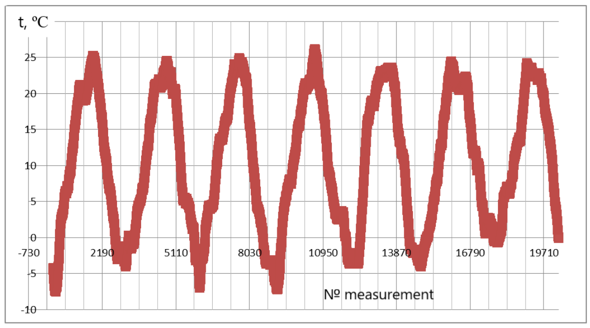

(c) 1 month

Figure 10. Average temperature values calculated with different duration of the integration interval

Analysis of these graphs showed that the amplitude of oscillations and extrema were shifted and depended on the integration period. In Figure 11, these curves are superimposed. It represents the increase in the amplitude of change of average temperature values and extreme values shift when reducing the integration period.

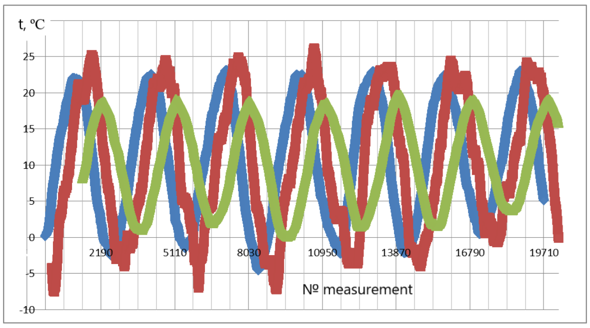

Figure 11. Average temperature values (integration period: 6 months - green curve, three months - blue, one month - red)

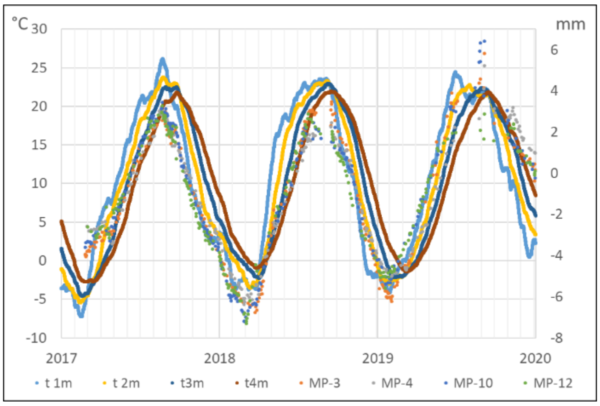

Figure 12. Average temperature values (1, 2, 3, 4 months) and horizontal displacements of points MP-3, MP-4, MP-10 and MP-14

The following objectives of the study were to establish a relationship between the mean integral values of temperature and the horizontal displacements of the dam control points. With this, a graph was created (Figure 12), in which solid curves indicate the average temperature values with different integration periods (1, 2, 3, 4 months) and dots present horizontal offset four points located in different parts of the dam (MP-3, MP-4, MP-10 and MP-14, see Figure 4). The main y-axis shows the average temperature values in°C and on the additional y-axis (point on the right) offset in millimetres.

According to studies conducted in Tretyak and Palianytsia (2021), the extreme values of the curve of the average temperature value become later than the curve of the approximate temperature values.

Selection of the proportional relationship between the primary and secondary axes (Figure 12) helps to find out that 1 month integration period is the best of the studied periods corresponding to the nature of the change in the horizontal displacements of the control points.

Further, the curve of change of average integrated values of temperature was compared with the integration period of 1 month and horizontal displacements of control points of the dam (Figure 13).

The graph shows the control points located on the dam. They change their position synchronously and relatively to the change in the average temperature. The only exceptions are point MP-2, whose amplitude of change of horizontal displacements is significantly bigger, and point MP-4, whose amplitude of change of horizontal displacements is slightly smaller than at other control points, especially in summer.

In Figures 12 and 13, the right vertical axes were selected to visualize the relationship between temperature and horizontal displacements of the control points. The actual relationship between these values is presented in Table 2.

Table 2. Coefficients of equations

Control point name	Coefficients of equations of horizontal displacements	
	a	*k*
MP-1	0.443	-5.590
MP-2	0.444	-2.555
MP-3	0.378	-5.222
MP-4	0.311	-4.889
MP-5	0.333	-3.667
MP-6	0.312	-3.869
MP-7	0.311	-3.868
MP-8	0.332	-3.666
MP-10	0.356	-4.445
MP-11	0.355	-3.444
MP-12	0.310	-3.869
MP-13	0.443	-5.590
MP-14	0.399	-5.002
MP-15	0.400	-5.000
Average values	**0.366**	**-4.334**

The amplitudes of the maximum horizontal displacements at each GNSS control point were further calculated. Figures 14 and 15 present the diagrams of annual maximum amplitudes of horizontal displacements recorded at different times of the year. Diagrams show that the maximum amplitudes of horizontal displacements in winter were recorded in 2018, and the minimum – in 2017. In the middle of the dam, there was a specific subsidence, i.e. the amplitudes of the horizontal displacements were smaller than at the edges of the dam.

The maximum summer amplitudes of horizontal displacements were recorded in 2019, and the minimum at most points – in 2018. The only exception is the amplitude at point MP-8. Only in 2019, the amplitude of horizontal displacements in the middle of the dam was smaller than at the edges.

Graphs in the Figure 16 show the epochs (ordinate axis containing days from the beginning of the year when the maximum displacements were observed) at each point. The epochs of maximum displacements in winter and summer in the middle of the dam occur later than at its edges, although the displacements themselves are opposite in sign.

Based on the data obtained and graphically presented in Figure 13, we established a linear relationship between the average temperature t and the horizontal displacements $\Delta(T)_i$ in the analytical form:

$$\Delta(T)_i = a \cdot t_{avg} + k \quad (2)$$

where: $\Delta(T)_i$ – horizontal displacement of the control point, t_{avg} – the average air temperature value for the previous lunar period.

Values *a* and *k* were determined for each control point and are shown in Table 2.

Based on the average values, we obtain the expression:

$$\Delta(T)_i = 0.37 \cdot t_{avg} + 4.33 \quad (3)$$

According to Formula (2) and the coefficients given in Table 2, it is possible to predict the value of the horizontal displacement of the control points installed on the ridge of the HPP, according to the measured air temperature value. Furthermore, Formula (3) helps to anticipate the value of the average horizontal offset of the items presented in the table.

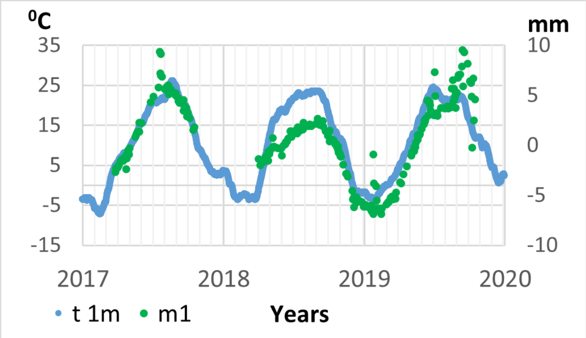

(a) control point MP-1

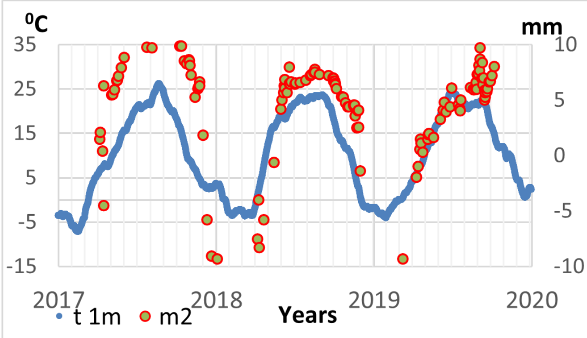

(b) control point MP-2

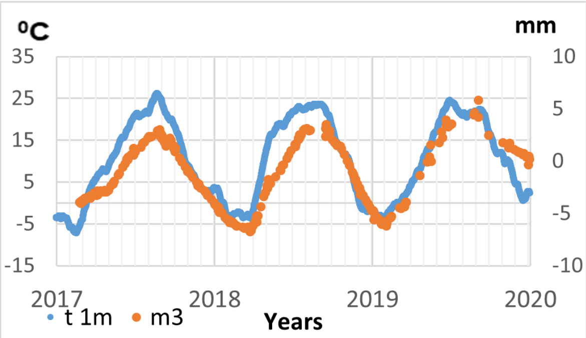

(c) control point MP-3

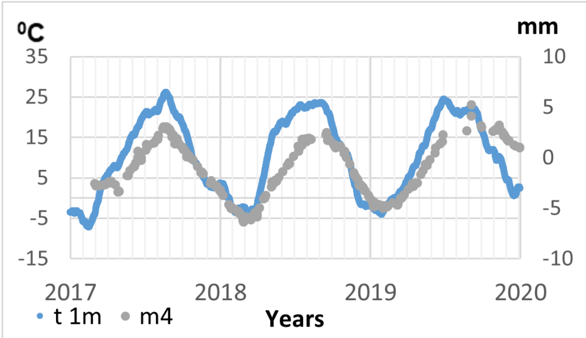

(d) control point MP-4

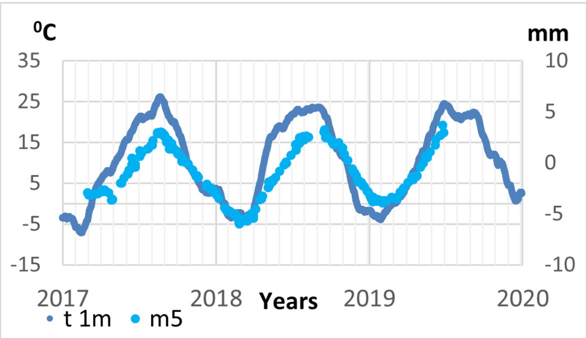

(e) control point MP-5

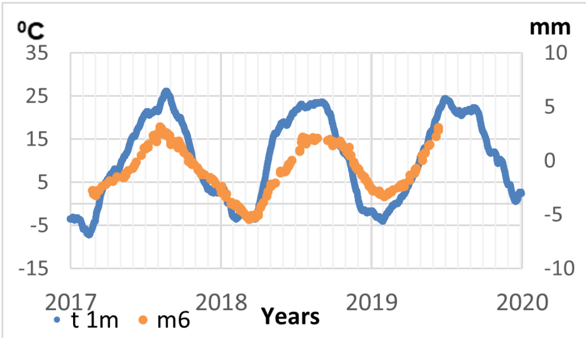

(f) control point MP-6

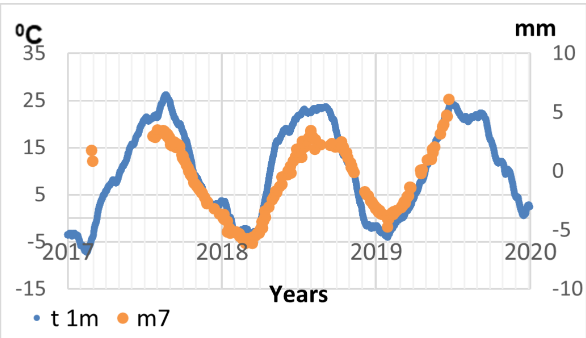

(g) control point MP-7

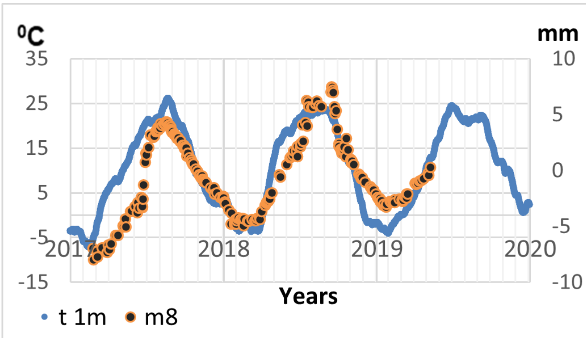

(h) control point MP-8

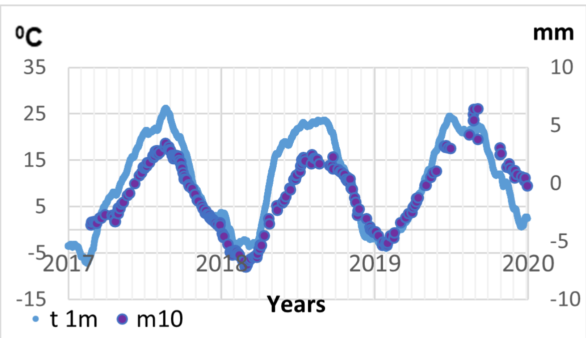

(i) control point MP-10

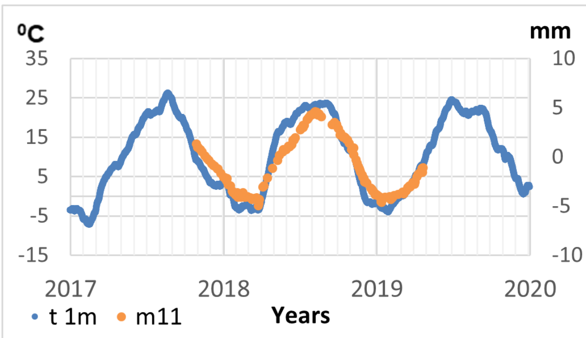

(j) control point MP-11

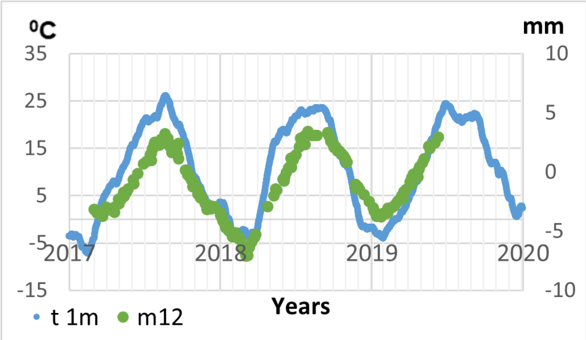

(k) control point MP-12

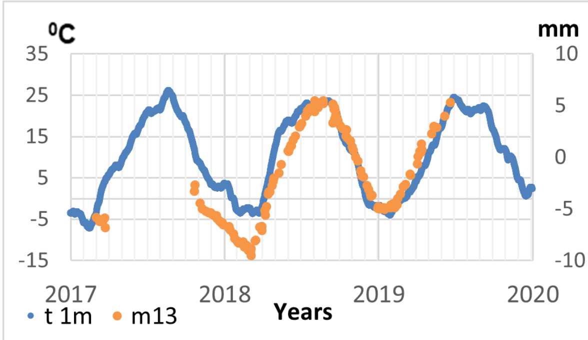

(l) control point MP-13

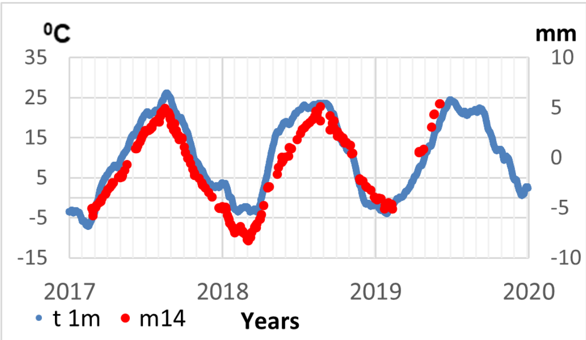

(m) control point MP-14

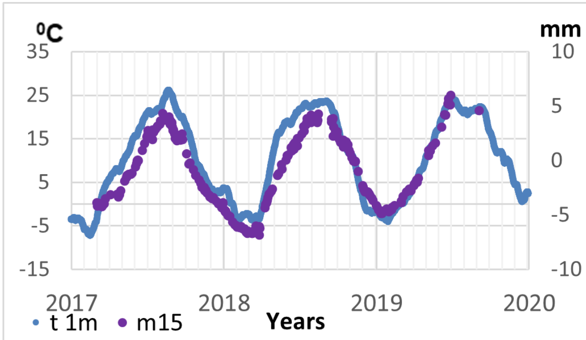

(n) control point MP-15

Figure 13. Average values of temperature (1 month) and horizontal displacements of GNSS control points

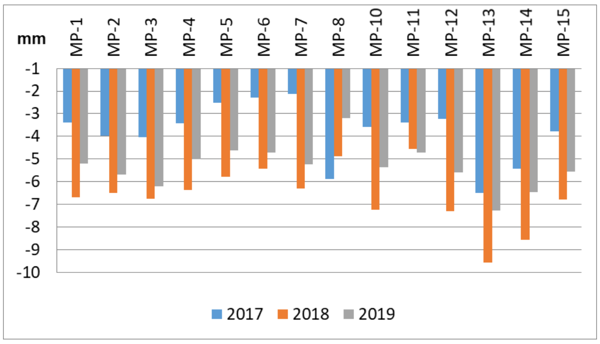

Figure 14. Values of amplitudes of horizontal displacements recorded in winter

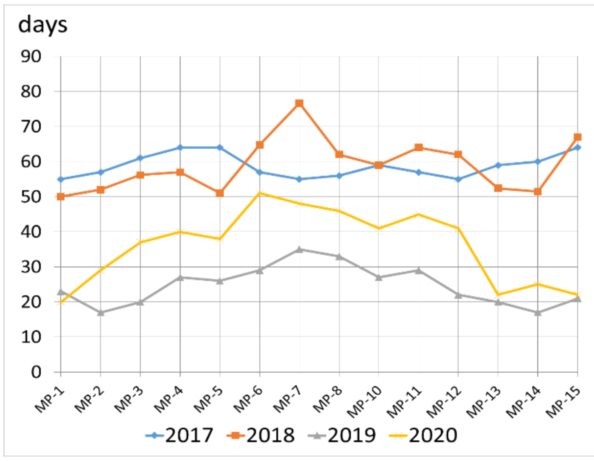

(a) winter

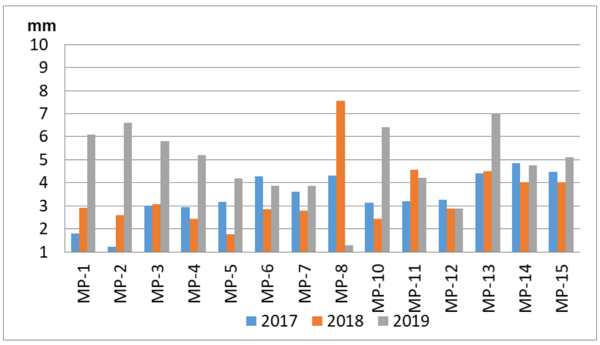

Figure 15. Values of amplitudes of horizontal displacements recorded in summer

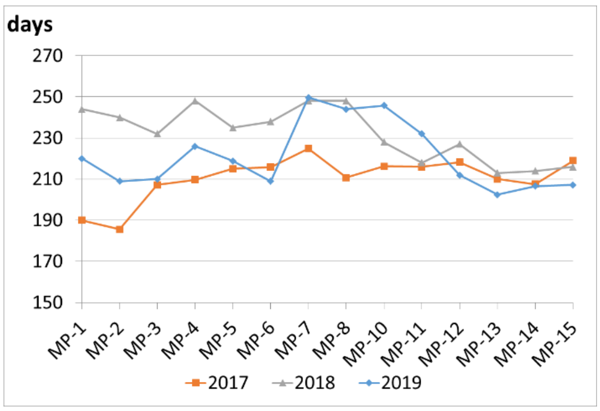

(b) summer

Figure 16. Epochs of maximum horizontal displacements of GNSS control points

The conducted researches allow establishing the values of seasonal deformations of the Dnieper Hydroelectric Station dam and the influence of air temperature on them. These deformations significantly impact the appearance of cracks in the dam's body and its stability. The magnitude of extreme displacements and the epoch of their manifestation depend on the dam's design and technical parameters. For each dam, these extreme displacements and the epochs of their manifestation will be different. Accordingly, monitoring these displacements and their changes over time is one of the criteria for assessing the general condition of the dam.

5 Scientific novelty and practical significance

The research result represents the regularities of the connection between the temperature change and the displacements of the GNSS points. It can be used for further research on the processing and analysis of the monitoring data of engineering constructions.

6 Conclusions

Based on the research, the following conclusions can be drawn.

1. The horizontal displacements of the first half of each year are opposite to ones recorded in the second half. In the first half of the year, the dam's body is shifted towards the reservoir, and in the second half of the year, in the direction of the lower reaches.
2. It is established that the projections of velocity vectors of reference points in the ETRF-2014 system for the studied period do not exceed the absolute value of 3 mm/month. The average displacement speed of the checkpoints installed on the dam is 1.4 mm/month in the northern and eastern directions.
3. In the absence of significant changes in the water level in the upper reservoir, ambient temperature has a decisive influence on the seasonal displacements of dams.
4. The epochs of maximum displacements in winter and summer come later in the middle part of the dam than on the extreme ones, even though the displacements themselves are opposite in sign.
5. Obtained data established a linear relationship between the average temperature and the horizontal displacements of the GNSS control points installed on the dam of the Dnieper Hydroelectric Station.
6. According to the three-year GNSS monitoring of the Dnieper Hydroelectric Station dam, the amplitude of semi-annual horizontal oscillations of the control points relative to the dam axis is from -9.5 to +8 mm. In winter and summer, the horizontal displacements increase from the edges of the dam to its central part. However, the amplitudes of the horizontal displacements shift the other way round. The maximum amplitudes of horizontal displacements in winter periods were recorded in 2018, and the minimum - in 2017, in summer periods, the maximum was in 2019, and the minimum at most points - in 2018.
7. The increase also influences the magnitude of the displacements in ambient temperature. Probably, in the central part of the dam, these temperature differences are much more significant, so in the middle of the dam, larger amplitudes of winter and summer vertical displacements are recorded.
8. The magnitude of extreme displacements and the epoch of their manifestation depend on the dam's design and technical parameters. For each dam, these extreme displacements and the epochs of their manifestation will be different. Accordingly, monitoring these displacements and their changes over time is one of the criteria for assessing the general condition of the dam.

References

(2020). Action plan for adaptation to the effects of climate change in the city of Zaporizhia. The project was approved by the decision of the 50th session of the City Council No. 38 from 3.06.2020. Last accessed January 2022.

Chrzanowski, A., Szostak, A., and Steeves, R. (2011). Reliability and efficiency of dam deformation monitoring schemes. In *Proceedings of the 2011 Annual Conference of Canadian Dam Association (CDA/ACB), Fredericton, NB, Canada, 15 October 2011*, volume 15.

Corsetti, M., Fossati, F., Manunta, M., and Marsella, M. (2018). Advanced SBAS-DInSAR technique for controlling large civil infrastructures: An application to the Genzano di Lucania dam. *Sensors*, 18(7):2371, doi:10.3390/s18072371.

Drummond, P. (2010). Combining CORS Networks, Automated Observations and Processing, for Network RTK Integrity Analysis and Deformation Monitoring. In *Proceedings of the 15th FIG Congress Facing the Challenges, Sydney, Australia, 11–16 April 2010*, pages 11–16.

Kang, F. and Li, J. (2020). Displacement model for concrete dam safety monitoring via gaussian process regression considering extreme air temperature. *Journal of Structural Engineering*, 146(1):05019001, doi:10.1061/(ASCE)ST.1943-541X.0002467.

Kuzmanovic, V., Savic, L., and Mladenovic, N. (2013). Computation of thermal-stresses and contraction joint distance of rcc dams. *Journal of Thermal Stresses*, 36(2):112–134, doi:10.1080/01495739.2013.764795.

Léger, P. and Leclerc, M. (2007). Hydrostatic, temperature, time-displacement model for concrete dams. *Journal of engineering mechanics*, 133(3):267–277, doi:10.1061/(ASCE)0733-9399(2007)133:3(267).

Mata, J., Tavares de Castro, A., and Sá da Costa, J. (2013). Time-frequency analysis for concrete dam safety control: Correlation between the daily variation of structural response and air temperature. *Engineering Structures*, 48:658–665, doi:10.1016/j.engstruct.2012.12.013.

Milillo, P., Bürgmann, R., Lundgren, P., Salzer, J., Perissin, D., Fielding, E., Biondi, F., and Milillo, G. (2016). Space geodetic monitoring of engineered structures: The ongoing destabilization of the mosul dam, iraq. *Scientific reports*, 6(1):37408, doi:10.1038/srep37408.

Moroko, V. (2010). *Dniproges: Black August 1941*. Scientific works of the historical faculty of Zaporizhia National University.

Oro, S., Mafioleti, T., Chaves Neto, A., Garcia, S., and Neumann, C. (2016). Study of the influence of temperature and water level of the reservoir about the displacement of a concrete dam. *International Journal of Applied Mechanics and Engineering*, 21(1):107–120, doi:10.1515/ijame-2016-0007.

Santillán, D., Salete, E., and Toledo, M. (2015). A methodology for the assessment of the effect of climate change on the thermal-strain-stress behaviour of structures. *Engineering Structures*, 92:123–141, doi:doi.org/10.1016/j.engstruct.2015.03.001.

Scaioni, M., Marsella, M., Crosetto, M., Tornatore, V., and Wang, J. (2018). Geodetic and remote-sensing sensors for dam deformation monitoring. *Sensors*, 18(11):3682, doi:10.3390/s18113682.

Tretyak, K. and Palianytsia, B. (2021). Research of seasonal deformations of the dnipo hpp dam according to gnss measurements. *Geodynamics*, 30(1):5–16, doi:10.23939/jgd2021.01.005.

Tretyak, K., Periy, S., Sidorov, I., and Babiy, L. (2015). Complex high accuracy satellite and field measurements of horizontal and vertical displacements of control geodetic network on dniester hydroelectric pumped power station (hpps). *Geomatics and environmental engineering*, 9(1):83–96, doi:10.7494/geom.2015.9.1.83.

Yigit, C. O., Alcay, S., and Ceylan, A. (2016). Displacement response of a concrete arch dam to seasonal temperature fluctuations and reservoir level rise during the first filling period: evidence from geodetic data. *Geomatics, Natural Hazards and Risk*, 7(4):1489–1505, doi:10.1080/19475705.2015.1047902.

Zhang, Y., Yang, S., Liu, J., Qiu, D., Luo, X., and Fang, J. (2018). Evaluation and analysis of dam operating status using one clock-synchronized dual-antenna receiver. *Journal of Sensors*, 2018:9135630, doi:10.1155/2018/9135630.